Published in final edited form as:
Heart Rhythm. 2008 July ; 5(7): 981–991. doi:10.1016/j.hrthm.2008.03.062.

Detection of the Diastolic Pathway, Circuit Morphology and Inducibility of Human Post-Infarction Ventricular Tachycardia from Mapping in Sinus Rhythm. Ciaccio, Detection of the VT Diastolic Pathway

Edward J Ciaccio, PhD[1,2], **Anthony W Chow, MD, FRCP**[3], **Riyaz A Kaba, MRCP**[1,3], **D Wyn Davies, MD, FRCP, FHRS**[3], **Oliver R Segal, MRCP**[3], and **Nicholas S Peters, MD, FRCP, FHRS**[3]

1*Department of Pharmacology, Columbia University*

2*Department of Biomedical Engineering, Columbia University*

3*Department of Cardiology, Saint Mary's Hospital, Imperial College London*

Abstract

Aims—We sought to determine whether sinus rhythm activation maps could be used to detect the origin and characteristics of reentrant ventricular tachycardia in postinfarction patients.

Method—In each of 11 post-MI patients, unipolar electrograms were acquired at 256 virtual endocardial sites using non-contact mapping. Electrograms were marked for activation time and mapped on a three-dimensional grid. Spatial differences in sinus-rhythm activation time were correlated to isthmus characteristics, and to activation through the diastolic pathway during tachycardia, based on presence of contiguous lines of slow conduction and block.

Results—Twenty tachycardia morphologies were analyzed. Fourteen sustained reentrant circuit morphologies occurred in 9 patients, with dual morphologies having a shared isthmus occurring in 5/9. Dual morphologies were caused by changes in entrance-exit point location about a common isthmus. One transient circuit morphology of <10 beats occurred in 3/9 patients also having sustained reentry. The estimated isthmus determined from sinus rhythm activation overlapped the diastolic pathway determined from tachycardia maps with 83.8% sensitivity and 89.2% specificity. Mean difference in sinus rhythm activation time across the isthmus border was larger in transient as compared to sustained morphologies (32.8±9.5ms versus 22.8±1.8ms), with smaller isthmus size (4.8±1.1cm^2 versus 10.0±1.1cm^2, $p<0.05$) narrower entrance-exit points (7.0±1.5mm versus 9.3 ±0.8mm, $p<0.05$), and greater activation time difference across them (16.3±3.5ms versus 10.1 ±1.0ms, $p<0.05$).

Conclusion—In post-MI patients, the reentry isthmus can be localized in the endocardial border zone from sinus rhythm activation maps. Nonsustained reentry occurs when isthmus size is small and entrance-exit points are narrow and more electrically discontinuous.

Corresponding Author: Edward J. Ciaccio, Ph.D., Department of Pharmacology, PH7W, Columbia University, 630 West 168th Street, New York, NY 10032, Electronic Mail: ciaccio@columbia.edu, Ph:212-305-5447, Fx: 212-342-0447.

The authors have no conflicts of interest to report.

Keywords

ablation; activation mapping; reentry; sinus rhythm; ventricular tachycardia

Background

Clinical ventricular tachycardia (VT) late after myocardial infarction is often caused by a reentrant circuit located in the infarct border zone (IBZ)[1]. The circuit usually originates from the subendocardial region although subepicardial substrates are possible[2]. In patients with tachycardia that is hemodynamically tolerated to allow mapping, prevention of recurrent VT is achieved by catheter ablation in approximately two-thirds of patients with a procedure-related mortality of 1–3%[3]. Mapping during VT to identify target regions for ablation can be difficult if VT is poorly tolerated or when it is noninducible. Procedural success is also diminished in substrates capable of generating complex circuits and/or multiple reentry morphologies[3]. Therefore, identification of critical parts of the reentrant circuit by mapping without VT induction is a desirable goal for catheter ablation therapy[1], which can potentially be enhanced by development of more accurate localization paradigms and increased understanding of reentry mechanisms. Recently we have shown in canine postinfarction hearts that large differences in sinus rhythm activation time at adjacent recording sites, termed electrical discontinuities, occur at the edge of the protected region of the reentrant circuit (diastolic pathway or reentry isthmus)[4]. These discontinuities define the pattern of activation through the diastolic pathway during reentry and are correlated to tachycardia duration in canine postinfarction ventricular tachycardia[4]. We used these methods to examine the relationship between electrical discontinuities in the endocardial border zone and reentrant circuit characteristics in postinfarction VT patients to address the hypothesis that the location and characteristics of the diastolic pathway in human VT can be detected from sinus rhythm activation time.

Method

Patient Inclusion Criteria

Noncontact data was obtained retrospectively from a consecutive series of 11 unselected patients with healed myocardial infarction, in whom the source of at least one VT morphology was endocardial reentry, as determined by inducibility using programmed stimulation and from noncontact maps[5,6] (Table 1). These patients underwent radiofrequency ablation with conventional 4-mm tipped catheters (nonirrigated) at St. Mary's Hospital (London, United Kingdom). All ventricular tachycardias that were analyzed in this series, both sustained and nonsustained, were reproducibly induced by programmed stimulation, all were clinically relevant and 19/20 of these were successfully targeted with catheter ablation to prevent recurrence. Conventional ECG criteria were used to predict the location of the ventricular tachycardia exit site of the reentrant circuit on the left ventricular endocardium. A train of 8 cycles was followed by decrementing extrastimuli (up to 2) until VT was induced or block occurred from local refractoriness. Guided by the noncontact isopotential maps and conventional entrainment criteria, single or multiple sites were selected for delivery of radiofrequency energy in order to render all clinical VT morphologies noninducible. The mean time to follow-up was 18.8±5.0 months, at which time there was no recurrence of targeted ventricular tachycardia in 10/11 patients.

Clinical Recordings and Data Reduction

Unipolar electrograms were acquired using a noncontact mapping catheter (EnSite 3000; Endocardial Solutions, Inc., St. Paul, MN, USA). The EnSite 3000 system incorporates a

multielectrode array (MEA) catheter, amplifier, and workstation[5–6]. The MEA consists of 64 wires attached to laser-etched electrodes and mounted on a 7.5-mL balloon. In the present study 70% of all measurements were <35mm from the center of the MEA and 90% were <45mm. Although minor inaccuracies in electrogram reconstruction occur with MEA to endocardium distances of <34mm, this error remains small with distances up to 50mm from the center of the array[5]. MEA electrical signals are amplified, sampled at 1.2 kHz, and filtered with a 0.1-300Hz passband [5–6]. From each pacing study, a subset of 256 virtual unipolar electrograms were exported as an ASCII data file for analysis and mapping. The 256 multichannel recordings were obtained as sixteen virtual electrogram sites separated by 11.25° of latitude along each of sixteen lines of longitude separated by 22.5°. The average distance between adjacent virtual recording sites on the heart surface was approximately 5mm although the spacing varied according to the shape of the heart and the polar coordinate location of the sites. Following data analysis, the map3d computer program was used to display each map point on a three-dimensional computerized grid according to its Cartesian coordinates[7].

Mapping activation in VT

For our retrospective clinical data analysis, VT events were subdivided into nonsustained (duration from onset to spontaneous termination <30s) and sustained (duration >30s). The VT cycle lengths were measured from the R-R interval of the electrocardiogram. To construct isochronal activation maps, custom-designed computer software was used to manually mark the intrinsic deflection of each unipolar electrogram at the point of sharpest slope, or at the approximate center point when multiple intrinsic deflections with sharp slopes were present[8]. Activation times referenced to the onset of the arbitrary time window of a representative cycle of VT were plotted on the computerized map grid, isochrones set at 20–50ms intervals, and arcs of conduction block were overlaid where wavefronts on opposite sides of the arcs moved in different directions[8].

Analysis of Sinus Rhythm Activation

All sinus rhythm recordings used for quantitative analysis were obtained without pacing the heart. The method for analyzing multichannel recordings obtained during sinus rhythm is illustrated in Figure 1. Panels A–B show the noncontact endocardial activation map of a selected patient during sinus rhythm (256 virtual sites in total) with anatomical locations noted. For clarity, activation times are only shown for a subset of all sites. Two large (i.e., >2 × 2cm) [4,–8] centers of late activation where reentry can potentially form are evident on the posterior endocardial surface, panel B (sites with encircled activation times). From each area of latest activation, arrows are drawn toward areas of earlier activation so that 4–7 recording sites on the computerized electrode grid reside adjacent to each arrow[9]. For any particular arrow, if only three successive sites in the same direction have activation times which progressively decrease, the arrow is drawn but it is extended to the nearest additional site in the same direction (four sites in all). If more than seven successive sites along the same direction have progressively decreasing activation time, the arrow is truncated at the seventh site. The arrows so formed are located in regions denoted by gray shading (Figure 1B).

The linear regression of activation times along each arrow is computed. An example of the computation is provided for the solid arrow that is overlapped on the map grid. Activation times for recording sites residing adjacent to it are 84, 77, 46, 17, and 5ms. The regression coefficient $r^2 = 0.97$ and the slope = 21.8ms. The average distance between the 256 virtual recording sites is ~5mm, therefore the activation gradient (AG) along this arrow is 0.23mm/ms. The activation gradient corresponds to the conduction velocity along the arrow if the activation wavefront is moving in the same direction as the arrow is pointing, which is usually the case. The regression analysis for all arrows is shown in Table 2. The basal region had slower mean activation gradient according to the slope of the regression line (0.34mm/ms) and a more

uniform progression of activation times according to r^2 (0.89) and p value (0.01). Since this region has relatively uniform slow conduction (USC), it was selected as being the most likely location at which an isthmus that is the source of ventricular tachycardia will form, in accord with a previous canine postinfarction study[9]. The regression line with both the slowest AG and largest r^2 as optimized from a two-dimensional scatterplot of r^2 versus p value is outlined in bold in Table 2 and it corresponds to the regression computed for the solid arrow on the map. This arrow is called the primary path, which is anticipated to approximately overlap the location where the isthmus of the reentrant circuit will form during ventricular tachycardia as described previously[9].

The algorithm used to delineate the reentry isthmus boundaries using the virtual noncontact unipolar recordings of activation time is similar to that which is used for analysis of the bipolar electrogram duration[9]. Locations within the USC region at which the difference in sinus rhythm activation time between any 2 adjacent sites was ≥15 ms were marked on the computerized map grid. Selected nodes were then connected to form the border of a contiguous region based on the following algorithm: (1) the region must overlap >50% of the primary path; (2) nodes were connected so as to (a) minimize the maximum distance between connections, followed by (b) minimization of the mean distance between connections; and (3) the inscribed region must have surface area ≥2.0 cm^2 (the approximate minimum isthmus surface area that was observed). The polygon so formed is the estimated isthmus, shown in Figure 1C as a thin solid line, with the nodes denoted by solid circles. Locations where functional block lines would be expected to form during reentry were drawn as thick black lines along segments of the polygon with ≥15 ms sinus rhythm activation time between the recording sites. The activation times at adjacent sites along the primary path can differ by > 15ms during sinus rhythm because conduction is uniform and slow. During reentrant tachycardia, such areas often form part of the isthmus boundary.

The sensitivity of the method for detecting isthmus location was calculated as the area of the actual isthmus that was overlapped by the estimated isthmus, divided by the area of the actual isthmus. The specificity was calculated as the area of the border zone that was not overlapped by the actual or estimated isthmus, divided by the area of the border zone that was not overlapped by the actual isthmus. Because we did not determine the boundaries of the border zone, we used a constant 5 × 5cm area as the approximate area of the border zone for all specificity calculations. For both actual and estimated isthmuses, the geometric centroid was calculated as the arithmetic mean of the set of coordinate points used to represent each surface on the computerized map grid. Measurements of area and their overlap were determined on the map grid using ImageJ (National Institutes of Health, Bethesda, MD). The mean sinus rhythm activation time difference about the entire actual isthmus perimeter, at reentry entrance and exit segments only, and at reentry block line segments only, was determined from activation maps and tabulated. Variables were summarized as mean ± standard error, and the unpaired t-test and One-Way ANOVA (SigmaStat ver. 3.11, 2004, Systat Software) were used to detect statistically significant differences ($p<0.05$). The fully automated sinus rhythm analysis technique requires less than 30 seconds of computation time per map on a PC-type computer.

Results

Clinical Characteristics

Table 1 shows the clinical characteristics and the anatomical locations of reentrant circuits for each patient. Patient number, gender, follow-up time, presence of ICD and drug administration, reentrant circuit morphology, circuit and ablation lesion location, and cycle lengths during sinus rhythm and during tachycardia are given. Sinus rhythm activation was constant from one cycle to the next over a period of many seconds. The first 9 patients had at least one mappable

reentrant circuit morphology; patients 10–11 had no mappable reentrant circuits. When reentrant tachycardia was mappable (patients 1–9) the circuit had a morphology of so-called double-loop reentry[6], and the mean distance between the edge of the isthmus and the closest ablation lesion was 11.3±2.9 mm.

VT was sustained with a mappable circuit morphology in 9 patients, with dual morphologies having a shared reentrant isthmus occurring in 5/9. Dual reentry morphologies in the same patient were distinguishable by changes in entrance and/or exit point location about the isthmus. A single non-sustained circuit morphology with distinct isthmus and diastolic pathway occurred in 3/9 patients in which sustained reentry was also inducible. In all VT activation maps, each circuit loop followed a progression of activation times; the time for traversal about each loop was in close correspondence to the tachycardia cycle length. In the sinus-rhythm endocardial activation maps of each patient, at least one large area of uniform slow conduction between regions of early and late endocardial activation occurred in regions that included both equatorial and polar locations.

Figure 2–Figure 3 show left ventricular endocardial activation maps for patient 5 with the distance scale given at the bottom. Figure 2A–B shows the endocardial activation map for an arbitrary sinus rhythm cycle prior to programmed electrical stimulation in this patient and is the same map as in Figure 1A–B. For selected sites denoted by circles in Figure 2B, virtual electrograms and the sinus rhythm ECG (mapped beat denoted by *) are shown in the insets to the right of the panel.

The sharpest small deflection in each electrogram trace was marked by hand as the activation time. Thus the signal resulting from near-field activation was marked rather than far-field activation from the entire ventricle. The uniform slow conduction region extends over an area that is several centimeters in length and width (Figure 2B and Figure 3B). Figure 2C–D shows the extrastimulation map with a coupling interval of 260ms that resulted in the reentrant tachycardia episode of panels E–F. Extrastimulation resulted in unidirectional block along a segment of the isthmus perimeter, which was followed by breakthrough to begin sustained reentrant tachycardia (Figure 2E–F). During reentry, the wavefront proceeds from north to south during tachycardia to enter the isthmus, or diastolic pathway (blue to red, Figure 2F). Exit from the isthmus occurred at several locations as denoted by arrows. Activation marks for the circled sites in panel F are shown in the inset to the right of the panel. The actual reentry isthmus boundary defining the diastolic pathway as determined from the tachycardia map is delineated by black lines. Thicker black lines show the location of functional conduction block during tachycardia. Thinner black lines delineate the isthmus perimeter elsewhere along its dimensions. There is approximate correspondence of isthmus, isthmus perimeter, and diastolic pathway entrance and exit point location as determined from the sinus rhythm estimate (gray) and from the actual VT map (black) when they are overlaid (F). The borders that identified the USC area during sinus rhythm had the greatest gradient of activation delay that corresponded to the isthmus during ventricular tachycardia, unlike other areas of slow conduction which had relatively more rapid activation time (compare Figure 2A–B and 2E–F).

Reentrant tachycardia with a differing circuit morphology was inducible in patient 5 which was generated by using a coupling interval of 220ms for extrastimulation, resulting in the formation of a long unidirectional block line (Figure 3D) as compared with extrastimulation at a longer coupling interval (Figure 2D). The two circuit morphologies mostly share a common isthmus and perimeter (Figure 2–Figure 3F) but differ in the length and location of entrance and exit points during reentry.

Both a sustained and a transient reentrant circuit morphology was inducible in patient 8 (Figure 4–Figure 5). The sinus rhythm map is shown in panels A–B of both figures. There is a single

region with uniform and markedly slow conduction (arrows, panels B) over an area that is several centimeters in length and width, not seen elsewhere in the endocardium. The regression for the primary path (solid black arrow) is shown at right in Figure 4. The stimulus site location at which VT was initiated was approximately the same for both circuit morphologies (Figure 4–Figure 5D); however the coupling interval for extrastimulation was 250ms for the sustained reentry morphology of Figure 4 and 500ms for the transient morphology of Figure 5. The shorter coupling interval resulted in the formation of an extended line of unidirectional block followed by breakthrough near the grid center (dotted arrow, Figure 4D). This resulted in sustained tachycardia with a stable cycle length of 321ms, and an actual reentrant diastolic pathway (enclosed black line, Figure 4F) that approximately overlapped the location of the sinus rhythm estimate shown overlapping (enclosed gray line). The unidirectional block line forming during extrastimulation was relatively short due to the long coupling interval when transient reentry was induced (Figure 5D,F). Tachycardia cycle length was long (487ms) due to presence of large areas of slow conduction near the isthmus.

Figure 6 shows the activation map for one of the patients in which tachycardia was inducible by programmed stimulation but a complete reentrant circuit was not mappable. No large region of uniform slow conduction as described by the criteria given in the Methods exists anywhere on the grid. The time for sinus rhythm activation across the endocardial surface was approximately 50ms, which was less than in patients having an entirely mappable reentrant circuit.

Summary Data

On average for this series of patients, five to six ablation lesions were made per case study and four to five of the lesions were made in proximity to the reentry isthmus location (Table 1). The location of functional block (thick curved black lines) and the direction of propagation through the diastolic pathway for one reentrant ventricular tachycardia morphology from each patient are shown in Figure 7. When multiple reentry morphologies occurred, each isthmus often approximately overlapped portions of the same area. Ablation lesion location in the vicinity of the isthmus for each patient is denoted by circles. In most cases, these lesions were both in close proximity to the isthmus and resulted in cessation of ventricular tachycardia without reinduction by programmed stimulation.

The estimated isthmus overlapped the actual isthmus with a sensitivity of 83.8% and specificity of 89.2% for the pooled data from all patients with a mappable reentrant circuit. The mean difference in the geometric centroid between estimated and actual isthmus locations was 8.9 ±1.2mm. At least part of a border of the VT circuit was accurately identified by areas of USC seen on SR mapping data and the geometric centroid was always located within the actual diastolic pathway thus potentially serving as a useful guide. Table 3 summarizes the characteristics of the reentry isthmus and its perimeter for all patients. The parameters are categorized according to their values for sustained reentrant tachycardia (14 morphologies), nonsustained reentry (3 morphologies), and tachycardia without a mappable circuit (2 morphologies) in the eleven postinfarction patients. According to Table 3, there are significant differences between several of the variables ($p<0.05$). Nonsustained tachycardias are driven by reentrant circuits in which the isthmus is smaller in surface area with narrower entrance and exit points and greater sinus rhythm discontinuities across its boundaries as compared to the substrate from which sustained tachycardias arise.

Discussion

The results of this study suggest that when reentrant ventricular tachycardia is caused by a reentrant circuit that is located entirely on the endocardial surface, its size, shape, and entrance and exit points to the diastolic pathway can be predicted from sinus rhythm analysis by finding

an endocardial region with uniform slow conduction. For sustained reentrant tachycardia, the uniform slow conduction region often has a surface area of >≈4cm^2 (Figure 2–Figure 4) in accord with previous results[4,8–9]. No such large region of uniform slow conduction during sinus rhythm was present in the two patients lacking a complete mappable reentrant tachycardia circuit. Furthermore, our results suggest that functional conduction block is important to reentry in clinical patients. Distinct reentrant tachycardia morphologies as defined by 12 lead ECG and cycle length, often share a common isthmus but differ in propagation direction and/or location across the isthmus perimeter during reentry, i.e., they differ according to which perimeter segments act as entrance and exit points. Some of the reentrant circuits that were mapped in this study were complex but all were approximately double-loop in form although both single-loop and four-loop[10] circuits have been observed elsewhere. In a previous retrospective clinical study we measured the sinus rhythm electrogram duration from noncontact recordings of post-MI patients to estimate reentry isthmus location[8]. However, activation time measurements, used in the present study, are more readily and rapidly calculated with computer software that is typically available to the clinical electrophysiologist. Furthermore, as shown in the current clinical study as well as in a previous canine postinfarction study[4], sinus rhythm activation time measurements are useful to measure the substantial differences in the reentry isthmus characteristics from which sustained versus nonsustained tachycardias originate. Prediction of the duration of a particular reentrant ventricular tachycardia morphology and thus its clinical relevance is therefore possible using measurements of activation time, the subject of future study.

Discontinuity at the isthmus boundaries

It is suggested from the results of this study and from a previous study in canine postinfarction hearts[4], that presence of electrical discontinuity about the diastolic pathway, which can be detected during sinus rhythm, is an important determinant of reentry. Slow conduction and block are likely to occur at the lateral edges of such regions particularly at short cycle lengths because they are high resistance interfaces which impede electrical conduction, and because an impedance mismatch occurs at their boundary with adjacent lower impedance areas[11–12]. Entrance and exit points to the path of diastolic activation through the reentry isthmus coincide with isthmus perimeter segments of lesser resistance where electrical conduction is less hindered at short cycle lengths[11–12]. At lines of functional block during reentrant VT, activation may actually be proceeding across the line very slowly, but it is stopped by the propagating wavefront that swings around to the other side the circuit loop[4]. Breakthrough at any point along the line will therefore become more likely if cycle length increases. During sinus rhythm, discontinuities become evident when the activation wavefront impinges upon them from the perpendicular, which tends to occur as the wavefront arrives from the normal zone to the infarct border zone at its edges, and then propagates inward towards the isthmus location[4].

When the isthmus perimeter discontinuity, and therefore resistance, is relatively large even at entrance and exit segments, the safety factor (SF) for conduction is likely to approach unity, increasing the potential for block on an early cycle at a point of entrance or exit to the isthmus[11–12]. The likelihood of early block which terminates tachycardia is exacerbated by a small isthmus surface area which reduces the pathlength for activation and therefore the time for recovery of excitability. Increased isthmus perimeter discontinuity and diminished isthmus size were characteristic of the transient reentrant circuit morphologies that occurred in this series of patients (Table 3). In contrast, lesser isthmus perimeter discontinuity magnitude at entrance-exit segments and their larger segment width would be expected to more likely result in sustained reentrant tachycardias due to the lesser resistance, lowered impedance mismatch, and therefore greater safety factor as the activation wavefront traverses the isthmus perimeter. For the two cases in which a complete reentrant circuit could not be mapped from the

endocardial surface virtual noncontact electrograms during ventricular tachycardia (Table 3), the isthmus surface area that was observable was only 4.11cm^2, suggesting that the potential circuit pathlength on the endocardium was less than the wavelength for activation[12]. Yet, if these tachycardias arose from reentrant circuits with midmyocardial components, then only portions of the characteristic changes in sinus rhythm activation time that delineate the reentry isthmus would be evident from the surface recordings.

Isthmus Characteristics

The results of our retrospective study compliment that of another clinical study of patients with structural heart disease[13], in which the VT origin was a macroreentrant circuit having one or two loops rotating about functional or anatomical conduction barriers, and in which the same reentry isthmus was shared by 2–4 circuit morphologies, with differences in entrance and exit point locations being the distinguishing factor between morphologies. The average isthmus dimension in these patients was 3.1cm × 1.6cm[13] whereas in our patient series it was 10.1cm^2 (~3.1cm × 3.1cm square) for sustained and 4.8cm^2 (~2.2cm × 2.2cm square) for transient reentrant tachycardia (Table 3). Hence, when complete endocardial reentrant circuits are mappable in human postinfarction patients, similar characteristics of isthmus size and changes in entrance and exit point location at a stationary isthmus perimeter, pertaining to changes in circuit morphology, can be observed and measured. The relationships of isthmus perimeter to reentry duration and form that we found are also similar to those demonstrated in a canine postinfarction study of two-dimensional circuits residing in the epicardial border zone[4]. Since a single ablation lesion at an entrance or exit point to the reentry isthmus can prevent reinduction of multiple reentrant circuit morphologies in canine infarct border zone1[4], prevention of reinduction of multiple clinical reentrant circuit morphologies with a single lesion may be possible using sinus rhythm map-guided catheter ablation. By predicting from sinus rhythm analysis the precise location and boundaries of the USC region at which a reentrant circuit is most likely to form, it may be possible to perform targeted ablation that will prevent reentrant tachycardia that may originate from a particular region of the heart, both existing and preventatively. The value of sinus rhythm map-guided catheter ablation also stems from the fact that it provides a complete map of the endocardial substrate so that lesions can be placed to minimize the possibility that new or modified reentrant circuits will occur from the anatomical block lines that are produced. This may reduce medium/long term ventricular tachycardia recurrences and the need for follow-up, a subject of future study.

Nonmappable Tachycardia

Two tachycardia episodes that were mapped based on activation time did not exhibit a complete endocardial reentrant circuit in the surface maps, yet the tachycardias were inducible and terminated via programmed electrical stimulation. Although the isthmus perimeters as mappable from the endocardial surface during sinus rhythm only averaged 4.11cm^2 for these two cases (see Table 2), if tachycardia was actually three-dimensional, then entrainment from surface stimulation would be expected to occur at a surface entrance or exit point to that three-dimensional isthmus. Ablation at such areas would potentially block the impulse at an entrance or exit point to prevent reinduction of the tachycardia morphology. This was also confirmed by conventional contact mapping data, and it is likely that the location of the critical isthmus responsible for maintaining VT had a deep intramural or epicardial location.

Comparison to Other Mapping Methods

In patients with structural heart disease, entrainment mapping remains the gold standard for defining the protected isthmus and other components of the VT circuit, yet successful ablation of reentry is achieved in only 60–90% of cases[15]. Frequent recurrences of VT despite implantable cardioverter-defibrillator (ICD) and antiarrhythmic drug therapy are a typical

indication for catheter ablation[16]. The sinus rhythm analyses already developed by other clinical investigators have met with some success for improving reentrant VT ablation accuracy in post-MI patients, but have largely been empirically guided by non-specific features such as low-voltage regions, electrically unexcitable scar, and localization of late sinus rhythm electrogram components[17].

In Figure 2–Figure 3 and Figure 4–Figure 5, sinus rhythm activation is late within or near the isthmus location in accord with previous clinical[5,8,17] and canine[4,9,14] investigations of postinfarction reentrant ventricular tachycardia. Late sinus rhythm activation at the isthmus is probably associated with the presence of the thinnest border zone which has been observed to occur at these areas[18–20]. Since tissue resistivity is anticipated to increase in proximity to the infarct[19–20], wavefront propagation would be expected to be slowed at the isthmus location during sinus rhythm, causing delayed activation there. In patients with infarct-related VT, noncontact mapping-guided ablation is associated with a high acute success rate, yet only 42.5% of patients remain free from VT/VF three years after ablation[21]. The extent and complexity of the scar-related arrhythmic substrate and potential for reentrant circuits likely contributes to the difficulty in achieving permanent freedom from tachycardia[22].

Sinus rhythm mapping can potentially improve outcome, particularly in cases where induced tachycardia is poorly tolerated or non-sustained, and possibly identify the regions of activation complexity that have characteristic properties, precisely identifying them as arrhythmogenic for tachycardia[23]. By our technique, better understanding and characterization of activation in sinus rhythm has revealed features that correlate specifically with the location of the reentrant circuit. This would be expected to be of benefit in both targeting ablation and to identify the target arrhythmogenic regions of the infarcted ventricle based on these criteria. Such left ventricular activation patterns may even identify and provide primary prevention in patients at risk of post-infarction reentry.

Several pacing and voltage mapping studies have described bystander areas (blind alleys or cul-de-sacs) which are not part of the actual reentry isthmus but have similar properties[3,17,22–23]. We believe these areas are potential substrates for reentry even though they do not participate in reentrant circuits that can be provoked during clinical study. Previous work has shown that multiple reentry morphologies often share a common isthmus location, and differ only in the exact path and the entrance and exit points[14,24]. In some instances, distinct substrates are responsible for differing reentry morphologies[24]. The method we describe herein selects the most likely isthmus location (i.e. the estimated isthmus boundary) and the direction of propagation during the diastolic interval of reentrant ventricular tachycardia (primary path) based on regression analysis. Other propagation directions (arrows of decreasing activation time, Figure 1 and Figure 4) and other potential isthmus locations (late activation area at Apex, Figure 2B) are possible and may correspond to bystander areas which are less likely to cause a particular clinical reentrant ventricular tachycardia morphology. Thus while our analysis does not directly differentiate isthmus from bystander regions, we believe that the bystander regions during one particular reentry morphology may be part of the circuit during other reentry morphologies[14,24].

Recently, Magnetic Resonance Imaging (MRI) has been used in canine postinfarction to measure changes in infarct border zone geometry for calculation of wavefront curvature[20]. Based on the methodology, functional block lines present during reentrant ventricular tachycardia were predicted to coincide with locations of abrupt increase from thin to thicker border zone tissue. As in canine postinfarction, sinus rhythm discontinuities and reentrant ventricular tachycardia characteristics in clinical postinfarction are likely affected by infarct border zone geometry[20], as well as changes in gap-junctional connections between myocytes[19], the subject of future study.

Limitations

This study was modeled after an analysis of sinus rhythm activation time in the canine postinfarction border zone[9]. However, canine infarct circuits are mostly two-dimensional, they are more commonly bounded by functional arcs of block, and they tend to be epicardial as compared with circuits in human postinfarction hearts which often have more anatomical components and reside at the endocardial surface and in the subendocardium. We modified the algorithm used to delineate the reentry isthmus based upon bipolar electrogram recordings in canine postinfarction, for analysis of virtual unipolar noncontact electrograms. The affect of differences in data characteristics, as well as any distortion during three-dimensional mapping, to determine best ablation sites for preventing clinical ventricular tachycardia must be validated in a prospective study. We quantified the clinical data retrospectively and hence double-blinded analysis was not possible in this study.

The diastolic pathway of the reentrant circuits that we analyzed were mostly constrained to the endocardium. However, mid- and epi-myocardial layers can be involved in the ventricular tachycardia circuit in the infarcted heart. The inverse solution and boundary element mathematics that are used to calculate virtual electrograms can detect activity in deeper layers as far-field deflections, much like conventional contact bipolar mapping. When the diastolic pathway is not constrained to the endocardium, far-field potentials corresponding to activity in distant myocardial layers may result, the subject of future research. Catheter ablation for infarct-related VT is an adjunctive therapy in patients with symptomatic VT[21,25] but has not been shown to be a complete substitute for ICDs and antiarrhythmic drugs. Ventricular scar[25] has not yet been reliably identified with noncontact electrograms which may be due to uncertainties in the virtual electrogram signal amplitude.

Conclusions

Analysis of noncontact activation maps acquired during normal sinus rhythm are useful to define the location and shape of the reentry isthmus that will occur during ventricular tachycardia in post-MI patients. The estimated isthmus boundary was derived from differences ≥15ms in sinus rhythm activation time at neighboring sites and was in agreement with the actual isthmus boundary during reentry. The estimated direction of propagation during the diastolic interval of reentry was delineated by the primary path and was in accord with the actual propagation direction. The algorithm used for estimating isthmus location, its boundaries, and propagation direction during the diastolic interval was essentially the same as that used previously for bipolar canine postinfarction recordings[9]. Additionally it was shown that nonsustained reentry tends to occur when isthmus size is relatively small and border discontinuities are large as described previously[4]. Although the location where ablation lesions should be positioned to stop reentrant ventricular tachycardia may be estimated from sinus rhythm analysis, prospective clinical evaluation will be necessary for evaluation.

Supplementary Material

Refer to Web version on PubMed Central for supplementary material.

Acknowledgements

Supported by National Institutes of Health-NHLBI Program Project Grant HL30557, and a British Heart Foundation Grant (RG/05/009, PS/98038).

References

1. Brunckhorst CB, Delacretaz E, Soejima K, et al. Ventricular mapping during atrial and right ventricular pacing: relation of electrogram parameters to ventricular tachycardia reentry circuits after myocardial infarction. J Interventional Cardiac Electrophysiology 2004;11:183–191.
2. Lacroix D, Klug D, Marquie C, et al. Identification of ventricular tachycardia of epicardial origin from unipolar potentials obtained at the endocardial surface: is it feasible? Pacing Clinical Electrophys 2002;25:1561–1570.
3. Stevenson WG, Delacretaz E. Strategies for catheter ablation of scar-related ventricular tachycardia. Current Cardiology Reports 2000;2:537–544. [PubMed: 11060581]
4. Ciaccio EJ. Ventricular tachycardia duration and form are associated with electrical discontinuities bounding the isthmus of the reentrant circuit. J Cardiovasc Electrophys 2005;16:646–654.
5. Schilling RJ, Davies DW, Peters NS. Characteristics of sinus rhythm electrograms at sites of ablation of ventricular tachycardia relative to all other sites: a noncontact mapping study of the entire left ventricle. J Cardiovasc Electrophysiol 1998;9:921–933. [PubMed: 9786073]
6. Schilling RJ, Peters NS, Davies DW. Simultaneous endocardial mapping in the human left ventricle using a noncontact catheter: comparison of contact and reconstructed electrograms during sinus rhythm. Circulation 1998;98:887–898. [PubMed: 9738644]
7. MacLeod, RS.; Johnson, CR. IEEE Eng Med Biol Soc 15th Annual International Conference. IEEE Press; 1993. Map3d: Interactive scientific visualization for bioengineering data; p. 30-31.
8. Ciaccio EJ, Chow AW, Davies DW, et al. Localization of the isthmus in reentrant circuits by analysis of electrograms derived from clinical non-contact mapping during sinus rhythm and ventricular tachycardia. J Cardiovasc Electrophysiol 2004;15:27–36. [PubMed: 15028069]
9. Ciaccio EJ, Tosti AC, Scheinman MM. Relationship between sinus rhythm activation and the reentrant ventricular tachycardia isthmus. Circulation 2001;104:613–619. [PubMed: 11479262]
10. Lin SF, Roth BJ, Wikswo JP Jr. Quatrefoil reentry in myocardium: an optical imaging study of the induction mechanism. J Cardiovasc Electrophysiol 1999;10:574–586. [PubMed: 10355700]
11. Spach MS, Miller WT III, Dolber PC, et al. The functional role of structural complexities in the propagation of depolarization in the atrium of the dog. Circulation Research 1982;50:175–191. [PubMed: 7055853]
12. Kléber AG, Rudy Y. Basic mechanisms of cardiac impulse propagation and associated arrhythmias. Physiol Rev 2004;84:431–488. [PubMed: 15044680]
13. de Chillou C, Lacroix D, Klug D, et al. Isthmus characteristics of reentrant ventricular tachycardia after myocardial infarction. Circulation 2002;105:726–731. [PubMed: 11839629]
14. Ciaccio EJ, Coromilas J, Costeas CA, et al. Sinus rhythm electrogram shape measurements are predictive of the origins and characteristics of multiple reentrant ventricular tachycardia morphologies. J Cardiovasc Electrophysiol 2004;15:1293–1301. [PubMed: 15574181]
15. Dixit S, Callans DJ. Mapping for ventricular tachycardia. Cardiac Electrophysiology Review 2002;6:436–441. [PubMed: 12438825]
16. Strohmer B, Hwang C. Ablation of postinfarction ventricular tachycardia guided by isolated diastolic potentials. Europace 2003;5:375–380. [PubMed: 14753635]
17. Stevenson WG. Catheter ablation of monomorphic ventricular tachycardia. Current Opinion Cardiol 2005;20:42–47.
18. Wit AL, Allessie MA, Bonke FI, et al. Electrophysiologic mapping to determine the mechanism of experimental ventricular tachycardia initiated by premature impulses. Am J Cardiol 1982;49:166–185. [PubMed: 6172033]
19. Peters NS, Coromilas J, Severs NJ, et al. Disturbed connexin43 gap junction distribution correlates with the location of reentrant circuits in the epicardial border zone of healing canine infarcts that cause ventricular tachycardia. Circulation 1997;95:988–996. [PubMed: 9054762]
20. Ciaccio EJ, Ashikaga H, Kaba RA, et al. Model of reentrant ventricular tachycardia based upon infarct border zone geometry predicts reentrant circuit features as determined by activation mapping. Heart Rhythm 2007;4:1034–1045. [PubMed: 17675078]
21. Segal OR, Chow AW, Markides V, et al. Long-term results after ablation of infarct-related ventricular tachycardia. Heart Rhythm 2005;2:474–482. [PubMed: 15840470]

22. Calkins H, Epstein A, Packer D, et al. Catheter ablation of ventricular tachycardia in patients with structural heart disease using cooled radiofrequency energy: results of a prospective multicenter study. Cooled RF Multi Center Investigators Group. Amer Coll Cardiol 2000;35:1905–1914.

23. Ellison KE, Stevenson WG, Sweeney MO, et al. Catheter ablation for hemodynamically unstable monomorphic ventricular tachycardia. J Cardiovasc Electrophysiol 2000;11:41–44. [PubMed: 10695460]

24. Costeas C, Peters NS, Waldecker B, et al. Mechanisms causing sustained ventricular tachycardia with multiple QRS morphologies: results of mapping studies in the infarcted canine heart. Circulation 1997;96:3721–3731. [PubMed: 9396476]

25. Bogun F, Marine JE, Hohnloser SH, et al. Relative timing of isolated potentials during postinfarction ventricular tachycardia and sinus rhythm. J Interventional Cardiac Electrophysiology 2004;10:65–72.

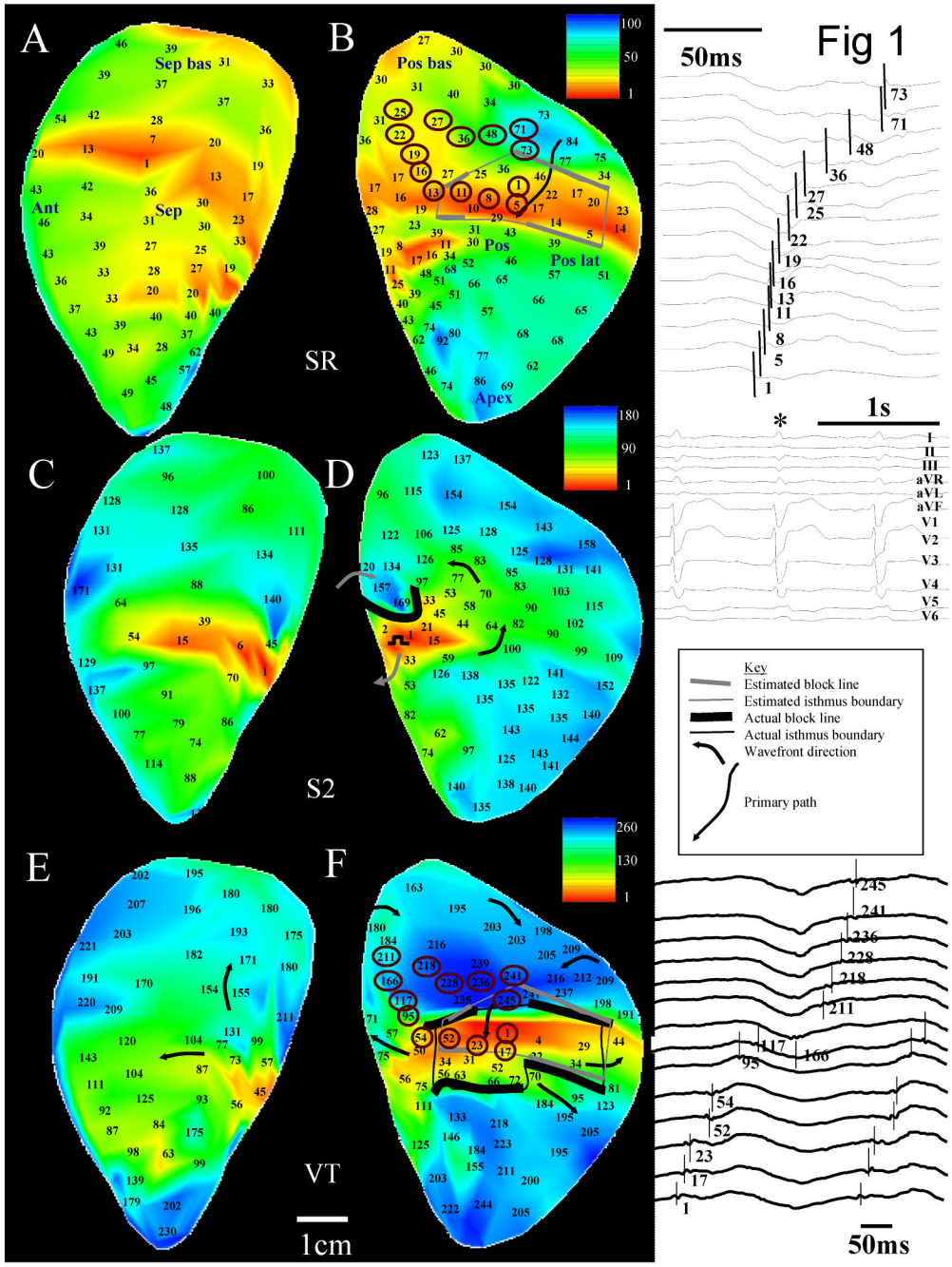

1.

Details of the methodology to determine the reentry isthmus perimeter by sinus rhythm and ventricular tachycardia activation mapping. For all activation maps, activation times are referenced to the earliest time on the grid which was set to 1ms.

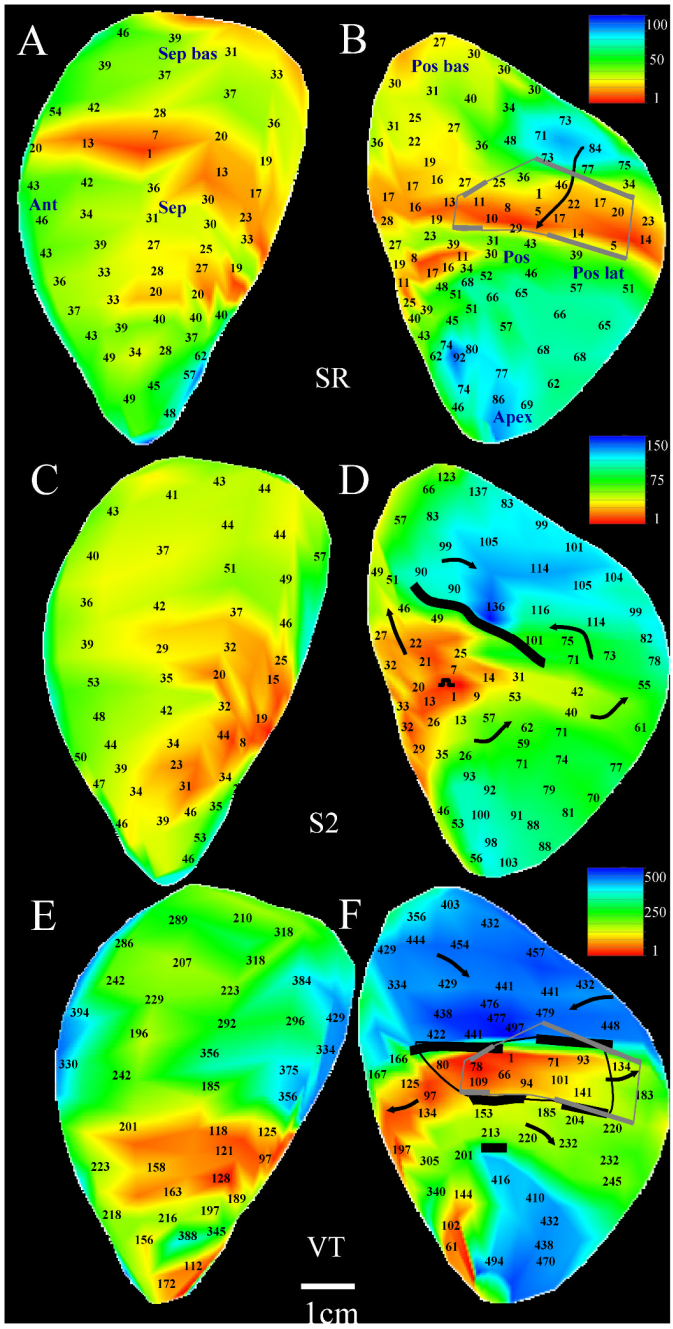

2.

Double-loop reentrant circuit and method to measure electrical discontinuity from Patient 5. Panels A–B: Sinus rhythm activation map and anatomical landmarks. Panels C–D: extrastimulation activation map. Panels E–F: sustained reentrant VT activation map. Estimated and actual isthmus perimeter and functional block line location are derived in panels B and F (gray and black lines, respectively). Insets to the right of maps (top to bottom): sinus rhythm electrograms that are circled in the map in panel B, ECG during sinus rhythm, key, and ventricular tachycardia electrograms at same location as shown in B.

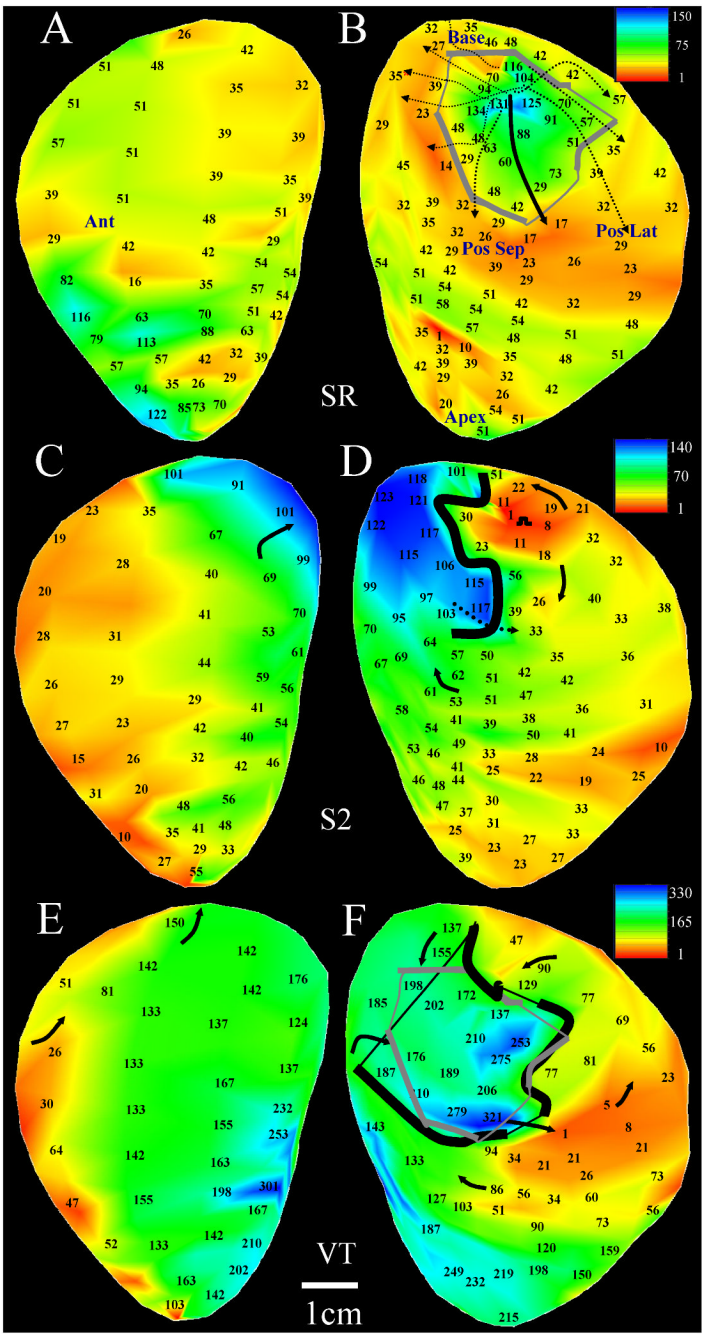

3.

Example of a reentrant circuit in Patient 5 with changes in the morphology of the circuit as compare to Figure 2E–F. Panels A–B: Sinus rhythm activation map (same as Figure 2A–B). Panels C–D: The extrastimulation cycle leading to the reentrant VT episode shown at the bottom of the figure. E–F: reentrant VT activation map. Arrows in the VT map denote the path of each loop of the circuit.

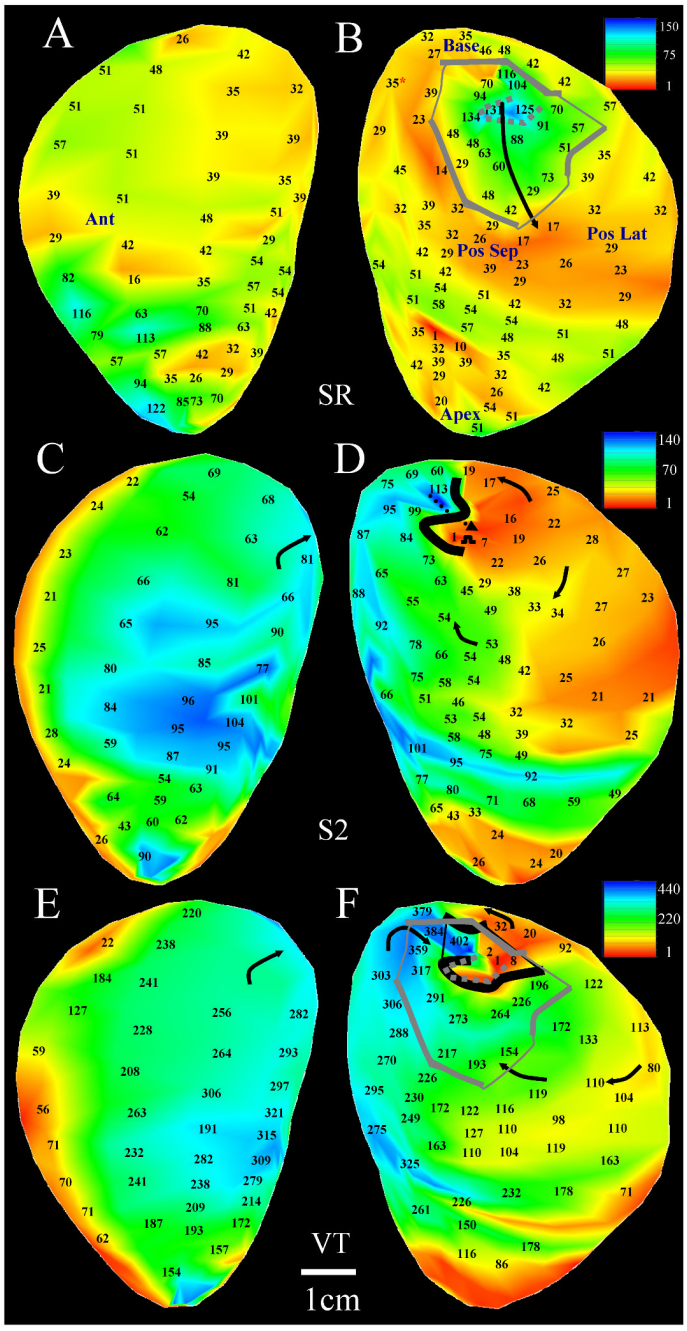

4.

Sustained double-loop reentry (Patient 8). A–B: sinus rhythm activation and anatomical landmarks. The measurements for predicting isthmus and block line location are shown adjacent to panel B. C–D: The extrastimulation cycle leading to the reentrant VT episode shown at the bottom of the figure. E–F: double-loop reentrant VT activation map with sinus rhythm estimate or isthmus perimeter location overlaid in gray.

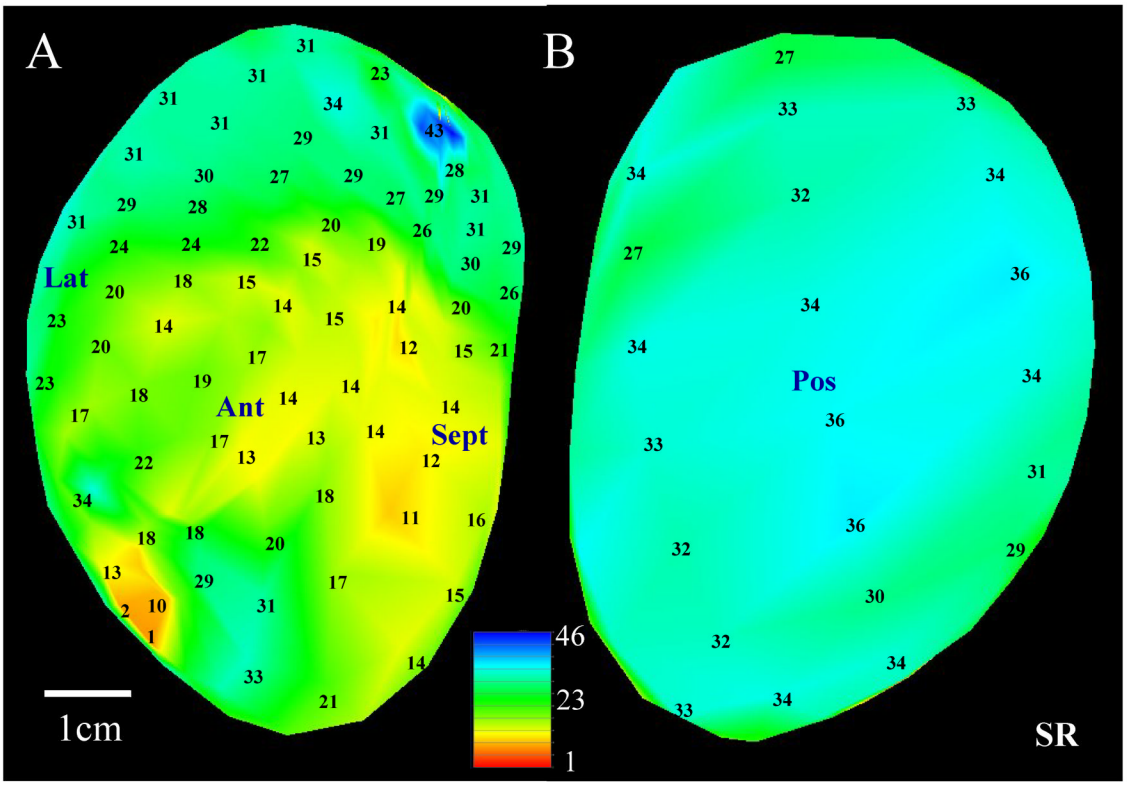

5.

Transient double-loop reentry (Patient 8). A–B: sinus rhythm activation map (same as Figure 4A–B). C–D: the extrastimulation cycle leading to the reentrant VT episode which was mapped as shown at the bottom of the figure. E–F: transient reentrant VT circuit. Note relatively small isthmus size and entrance point compared with sustained tachycardia episodes. Overlaid on this map is the sinus rhythm estimate of the isthmus perimeter (gray lines). Portions of the circuit boundary coincide with an additional area with sharp transition in sinus rhythm activation time (dotted gray line in panels B and F).

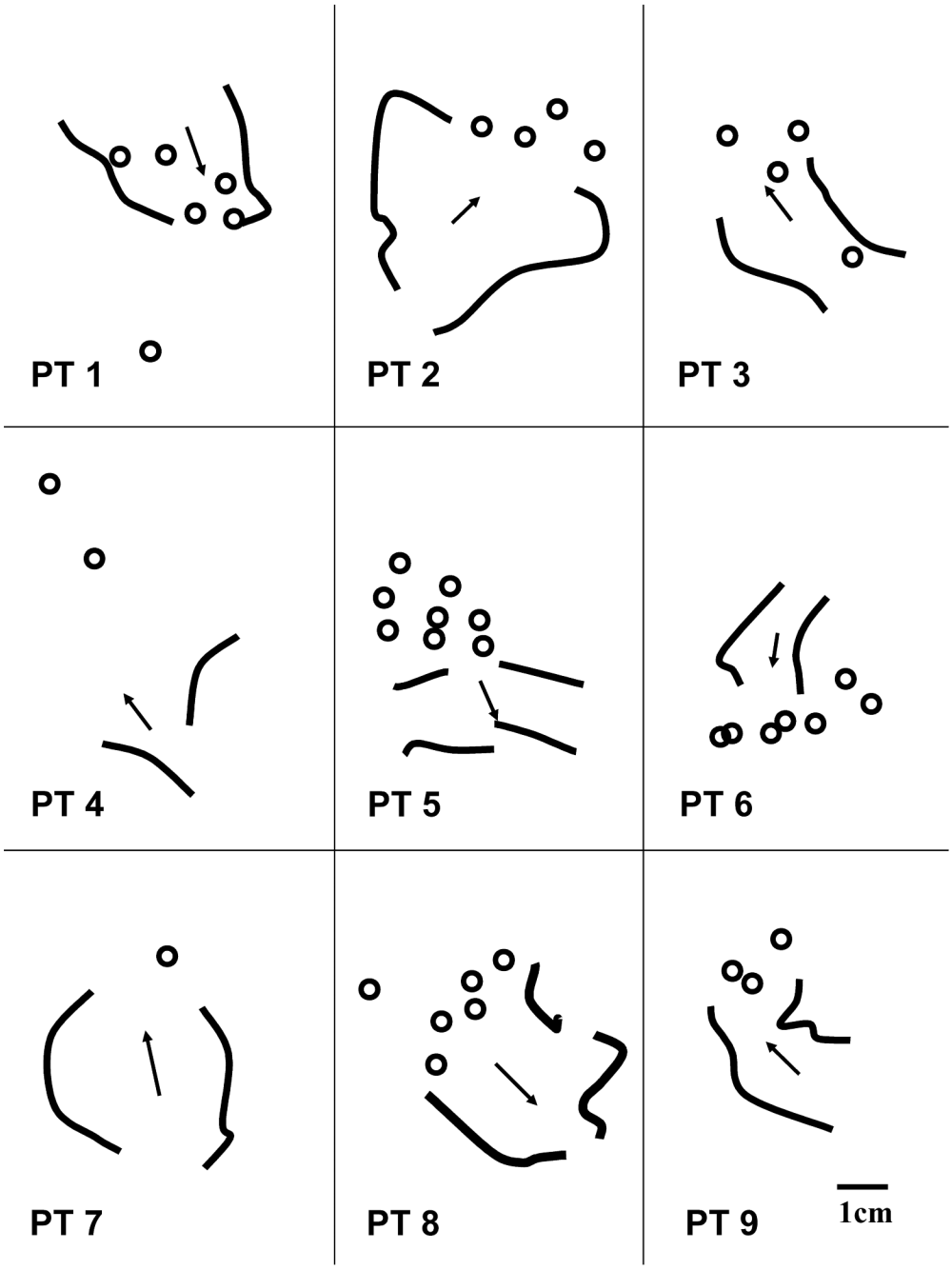

6.

Sinus rhythm activation map in patient lacking mappable reentrant circuit. Only a small area of uniform slow conduction was found to be present in this map, and activation of the entire endocardial surface is relatively rapid.

Table 1

Patient Clinical Data

Patient	Mph	Sex	Follow-up (mo)	ICD	Drug	Circuit	Abl	Abl loc	SR CL	VT CL
1	1	M	26	N	am	Ant	5/7	dp	696	407
2	1 2	M	18	Y	so	Ant	4/5	ex	910	459 271
3	1 2# 3	M	24	P	am	inf-lat	4/4	en, ex	1039	365 359 324
4	1	F	12	N	am	pos-inf	0/2	far ex	613	312
5	1* 2 3	M	25	Y	am + mex	Pos	8/8	en	831	465 294 581
6	1 2	M	13	Y	am + mex	Lat	7/7	ex	731	426 247
7	1	M	12	Y	am	Inf	1/1	ex	504	451
8 @	1# 2	M	20	N	am	pos-lat	6/9	en	653	487 321
9	1 2 3#	M	19	N	am	Ant	3/9	ex	736	424 314 340
10	1*	M	18	Y	am	Pos	-/1		787	280
11	1	M	20	Y	am	Ant	-/9		643	319
Mean	1.6		18.8				4.2/5.6		740.3	372.3

Mph: VT morphology, Follow-up: time from infarction to electrophysiologic study

ICD - implantable cardioverter-defibrillator, Y: yes, N: no, P: post ablation

Circuit: location of the isthmus of the sustained reentrant VT circuit

Abl: number of ablation sites within isthmus or near entrance-exit / all ablation sites

Abl loc: location of ablation lesions with respect to diastolic pathway

dp: centered within diastolic pathway, en: near the dp entrance, ex: near the dp exit, far ex: distant from the dp exit

SR CL: sinus rhythm cycle length in milliseconds

VT CL: ventricular tachycardia cycle length in milliseconds

transient

* complete reentrant circuit could not be mapped from activation times, am: amiodarone, so: sotalol, mex: mexiletine

@ Patient 8 (Figure 4–Figure 5) had recurrent VT after ablation

Table 2

Regression Analysis

Arrow	AG - BASE	r^2	p	AG - APEX	r^2	p
1	0.49	0.728	0.0310	0.81	0.584	0.2360
2	0.53	0.768	0.0220	0.46	0.909	0.001
3	0.32	0.977	0.001	0.60	0.699	0.1640
4	0.30	0.917	0.003	0.48	0.742	0.1390
5	0.29	0.959	0.001	0.46	0.609	0.2200
6	**0.29**	**0.970**	**0.001**	0.31	0.814	0.0980
7	0.25	0.834	0.0300	0.59	0.492	0.2990
8	0.29	0.921	0.004	0.41	0.969	0.002
MN±SE	0.34±0.039	0.89±0.034	0.011±.005	0.52±0.053	0.73±0.058	0.144±0.038

AG = activation gradient

Table 3

Isthmus Parameters

Parameter	Nonsus. Reentrant VT	Sus. Reentrant VT	Nonmappable VT
SR discontinuity- perimeter (ms)	32.83±9.51	22.78±1.83	23.42±5.95
Isthmus surface area (cm^2)	4.75± 1.06*	10.04± 1.09*	4.11± 0.41*
Width of entrance/exit (mm)	7.04±1.52**	9.30±0.75**	--
# entrance+exit points	2.00±0.00	2.71±0.19	--
SR discontinuity-entrance/exit (ms)	16.25± 3.48**	10.11±1.02**	10.75±2.78
Primary Path gradient (mm/ms)	0.22±0.06	0.32±0.02	0.33±0.03
Primary Path r^2	0.95±0.01	0.96±0.01	0.93±0.03

SR = sinus rhythm; ms = milliseconds; mm = millimeters, Nonsus = nonsustained, Sus = sustained

* $p < 0.05$, One-Way ANOVA

** $p < 0.05$, unpaired t-test